RESEARCH ARTICLE

Subcellular Investigation of Photosynthesis-Driven Carbon Assimilation in the Symbiotic Reef Coral *Pocillopora damicornis*

Christophe Kopp,[a] Isabelle Domart-Coulon,[b] Stephane Escrig,[a] Bruno M. Humbel,[c] Michel Hignette,[d] Anders Meibom[a,e]

Laboratory for Biological Geochemistry, School of Architecture, Civil and Environmental Engineering (ENAC), École Polytechnique Fédérale de Lausanne (EPFL), Lausanne, Switzerland[a]; MCAM UMR7245 CNRS-MNHN, Muséum National d'Histoire Naturelle, Paris, France[b]; Electron Microscopy Facility, University of Lausanne, Lausanne, Switzerland[c]; Aquarium Tropical, Établissement Public du Palais de la Porte Dorée, Paris, France[d]; Center for Advanced Surface Analysis, Institute of Earth Sciences, University of Lausanne, Lausanne, Switzerland[e]

ABSTRACT **Reef-building corals form essential, mutualistic endosymbiotic associations with photosynthetic *Symbiodinium* dinoflagellates, providing their animal host partner with photosynthetically derived nutrients that allow the coral to thrive in oligotrophic waters. However, little is known about the dynamics of these nutritional interactions at the (sub)cellular level. Here, we visualize with submicrometer spatial resolution the carbon and nitrogen fluxes in the intact coral-dinoflagellate association from the reef coral *Pocillopora damicornis* by combining nanoscale secondary ion mass spectrometry (NanoSIMS) and transmission electron microscopy with pulse-chase isotopic labeling using [^{13}C]bicarbonate and [^{15}N]nitrate. This allows us to observe that (i) through light-driven photosynthesis, dinoflagellates rapidly assimilate inorganic bicarbonate and nitrate, temporarily storing carbon within lipid droplets and starch granules for remobilization in nighttime, along with carbon and nitrogen incorporation into other subcellular compartments for dinoflagellate growth and maintenance, (ii) carbon-containing photosynthates are translocated to all four coral tissue layers, where they accumulate after only 15 min in coral lipid droplets from the oral gastroderm and within 6 h in glycogen granules from the oral epiderm, and (iii) the translocation of nitrogen-containing photosynthates is delayed by 3 h.**

IMPORTANCE **Our results provide detailed *in situ* subcellular visualization of the fate of photosynthesis-derived carbon and nitrogen in the coral-dinoflagellate endosymbiosis. We directly demonstrate that lipid droplets and glycogen granules in the coral tissue are sinks for translocated carbon photosynthates by dinoflagellates and confirm their key role in the trophic interactions within the coral-dinoflagellate association.**

Received 12 November 2014 **Accepted** 18 December 2014 **Published** 10 February 2015

Citation Kopp C, Domart-Coulon I, Escrig S, Humbel BM, Hignette M, Meibom A. 2015. Subcellular investigation of photosynthesis-driven carbon assimilation in the symbiotic reef coral *Pocillopora Damicornis*. mBio 6(1):e02299-14. doi:10.1128/mBio.02299-14.

Editor Margaret J. McFall-Ngai, University of Wisconsin

Address correspondence to Christophe Kopp, christophe.kopp@epfl.ch, or Anders Meibom, anders.meibom@epfl.ch.

Photosynthesis plays a central role in many aquatic animals symbiotically associated with microalgae or cyanobacteria (1). Shallow-water reef-building scleractinian corals hosting photosynthetic dinoflagellates of the genus *Symbiodinium* ("zooxanthellae") represent an emblematic example of such a stable mutualistic endosymbiotic relationship, which is critical for the development and health of coastal coral reef ecosystems in (sub)tropical oceans. The dinoflagellate endosymbionts, located within the coral gastrodermal cells (see Fig. S1 in the supplemental material), significantly contribute to the nutrition of their animal host partner by transferring a large fraction (up to 90%) of their photosynthetically assimilated carbon (C) and nitrogen (N) to support growth, respiration, reproduction, and biocalcification of the coral in nutrient-poor marine environments (2, 3). These photosynthates are produced by dinoflagellates through the fixation of dissolved inorganic carbon (DIC) via the Calvin-Benson "C3" photosynthetic pathway (4) and through the photosynthesis-dependent acquisition of dissolved inorganic nitrogen (DIN), ultimately via the glutamine synthetase-glutamate synthase (GS-GOGAT) enzymatic cycle (5, 6). The nature of translocated photosynthates ("mobile compounds") ranges from soluble low-molecular-weight compounds, such as glycerol, glucose, amino acids, and organic acids (7–9), to more complex molecules, such as free fatty acids (10) or glycoconjugates (11). However, the detailed pathway of this nutritional autotrophic flux from the dinoflagellate endosymbionts to the different cellular layers composing the coral host tissue, as well as the precise fate and turnover of photosynthates in the symbiotic system, remain poorly documented at the (sub)cellular level.

Symbiotic reef-building corals are regarded as "fat organisms" because they contain 9 to 47% (dry weight) lipids in their tissue, mostly in the form of neutral lipids (triglycerides, wax esters, and sterols) packed into lipid droplets (LDs), which are hypothesized to be a main sink for C-rich photosynthates translocated by dinoflagellates to the coral tissue (12–15). In support of this view, most previous bulk-level studies using radioactive (^{14}C) or stable (^{13}C) isotope labeling found preferential incorporation of translocated photosynthates into a chemically extracted lipid fraction, as well as structural polymeric compounds such as proteins (16–21). Additionally, recent observations indicate morphological and com-

positional changes of coral LDs upon coral bleaching (i.e., loss of dinoflagellates or their pigmentation) and a positive correlation between abundance of coral LDs and dinoflagellate density or light intensity (22, 23). Nevertheless, despite their supposed key role in the trophic interactions within the coral-dinoflagellate endosymbiosis, a direct demonstration that coral LD biosynthesis is linked with the release of photosynthates by dinoflagellates is still lacking.

Glycogen is another potentially important C reserve pool in the endosymbiosis, previously detected in stony corals both biochemically and ultrastructurally (24, 25). Gene expression for glycogen synthase and glycogen phosphorylase enzymes, which regulate the production and mobilization of glycogen stores, was detected in the reef coral *Acropora aspera* transcriptome (26). However, the possible incorporation of photosynthates such as glucose (9) into coral glycogen has not been investigated. Furthermore, little attention has been paid to the allocation and turnover of photosynthates within the dinoflagellate subcellular compartments, especially in their C storage structures, which are LDs and starch granules (27, 28).

Nanoscale secondary ion mass spectrometry (NanoSIMS) ion microprobe imaging is a powerful tool to simultaneously image and quantify the distribution and turnover of stable isotopic tracers (e.g., ^{13}C and ^{15}N) inside cells, especially when correlated with ultrastructural transmission electron microscopy (TEM) imaging (29–33). Here, we used this methodological approach on microcolonies (nubbins) of the common Indo-Pacific symbiotic reef-building coral *Pocillopora damicornis*, which were pulse-labeled in an aquarium for 6 h simultaneously with [^{13}C]bicarbonate and [^{15}N]nitrate ($^{15}NO_3^-$), followed by an extended chase of 186 h under either normal light/dark cycling (12 h/12 h) or prolonged darkness. We used [^{15}N]nitrate to unambiguously track the flow of N in the endosymbiotic system because nitrate is assimilated by the dinoflagellates only, in contrast to ammonium, the preferred source of DIN for most reef corals, which is simultaneously assimilated by both dinoflagellate and coral cells (32, 33).

The two main objectives of this study were to visualize and measure *in situ*, with subcellular resolution, the photosynthesis-dependent incorporation, fate, and turnover of inorganic C in the dinoflagellate endosymbionts and to track the translocation of dinoflagellate photosynthates toward the coral host tissue layers (see Fig. S1 in the supplemental material), especially their incorporation and turnover in coral LDs and glycogen granules.

RESULTS

Assimilation and turnover of carbon and nitrogen in dinoflagellates. NanoSIMS $^{13}C/^{12}C$ and $^{15}N/^{14}N$ isotopic images of dinoflagellate endosymbionts indicate spatially heterogeneous intracellular distribution of ^{13}C and ^{15}N incorporated during the 6-h labeling pulse under light (a representative dinoflagellate cell is illustrated in Fig. 1A to C). Regarding incorporated ^{13}C, preferential accumulation was systematically recorded on isotopic images in the following dinoflagellate compartments, identified on corresponding ultrastructural TEM micrographs and collectively termed "C reserves": (i) large, "primary" starch granules (terminology of Doyle and Doyle [27]) forming a cap around the plastidial pyrenoid (red arrows in Fig. 1A and B), (ii) small "secondary" starch granules distributed in the cytosol (blue arrows in Fig. 1A and B), and (iii) highly osmiophilic electron-dense LDs (green arrows in Fig. 1A and B).

NanoSIMS isotopic measurements from regions of interest (ROIs) defined in the dinoflagellate population (as illustrated in Fig. S2 in the supplemental material) show that the average ^{13}C enrichment of the dinoflagellate C reserves increased rapidly, after 15 min, during the 6-h labeling pulse under light, but then it declined by ~80% of its peak value, during the first 18 h of the chase under light/dark cycling, over a period that includes the first 12-h dark phase (Fig. 1D). (Summary data tables and *P* values from statistical analyses are provided in Data Set S1 in the supplemental material). In parallel, incorporated ^{13}C started to accumulate after 15 min into the pulse in the various other dinoflagellate compartments (e.g., nucleus and plastid) (Fig. 1A, B, and E). In contrast to C reserves, the ^{13}C enrichment of other compartments in the dinoflagellates only slowly decreased throughout the 186-h chase period, by about 60% of its peak value (Fig. 1E; see Data Set S1).

Regarding ^{15}N incorporated by the endosymbionts, this tracer was detected to accumulate in the dinoflagellate C reserves after 30 min into the pulse of labeling, but the ^{15}N enrichment in these compartments remained essentially stable during the chase (Fig. 1D). In the various other dinoflagellate compartments, ^{15}N was incorporated after 15 min into the pulse with a pattern of isotopic depletion throughout the chase almost identical to that of ^{13}C (Fig. 1E). Note that preferential incorporation of ^{15}N into vesicles containing uric acid crystals was confirmed (33, 34) (black arrows in Fig. 1A and C). Figure S3 in the supplemental material illustrates the turnover of both C and N during the pulse-chase experiment in representative dinoflagellates.

In corals maintained for 186 h in constant darkness, following the 6-h labeling pulse under light, the pattern of rapid ^{13}C decrease in the C reserves of dinoflagellates was confirmed (see Fig. S4 in the supplemental material). In addition, the observed ultrastructural changes indicate that both dinoflagellate LDs and starch granules were progressively depleted in the absence of photosynthetic carbon replenishment, an observation concomitant with the gradual appearance of ultrastructural symptoms of dinoflagellate cell degeneration (see Fig. S4). Severe paling of coral microcolonies was also noticed after this prolonged dark treatment (8 days), strongly suggesting that coral bleaching had occurred.

No significant incorporation of ^{13}C and ^{15}N was observed in dinoflagellate and coral cells pulse-labeled for 6 h in darkness following a 24-h pretreatment in darkness (see Fig. S5 in the supplemental material). This result confirms that C and N assimilation by dinoflagellates is light dependent (i.e., related to photosynthesis) and that the contribution of nonphotosynthetic "heterotrophic" C fixation by carboxylation reactions was negligible in both dinoflagellate and coral cells.

Translocation of carbon and nitrogen to the coral host tissue. At the overall coral tissue level, NanoSIMS isotopic measurements from ROIs (as illustrated in Fig. S2 in the supplemental material) demonstrate the gradual translocation of ^{13}C from the dinoflagellate endosymbionts to all four coral epithelia, starting after only 15 min and stabilizing after 48 h in the pulse-chase experiment with light/dark cycling (Fig. 2A, B, and D). (Summary data tables and *P* values of statistical analyses are given in Data Set S1 in the supplemental material, and Fig. S6 in the supplemental material illustrates a sequence of representative TEM and NanoSIMS isotopic images of the coral oral tissue.) Among the coral tissue layers, ^{13}C-labeled photosynthates transferred by dinoflagellates during the pulse were observed to rapidly (within 15 min) accumulate

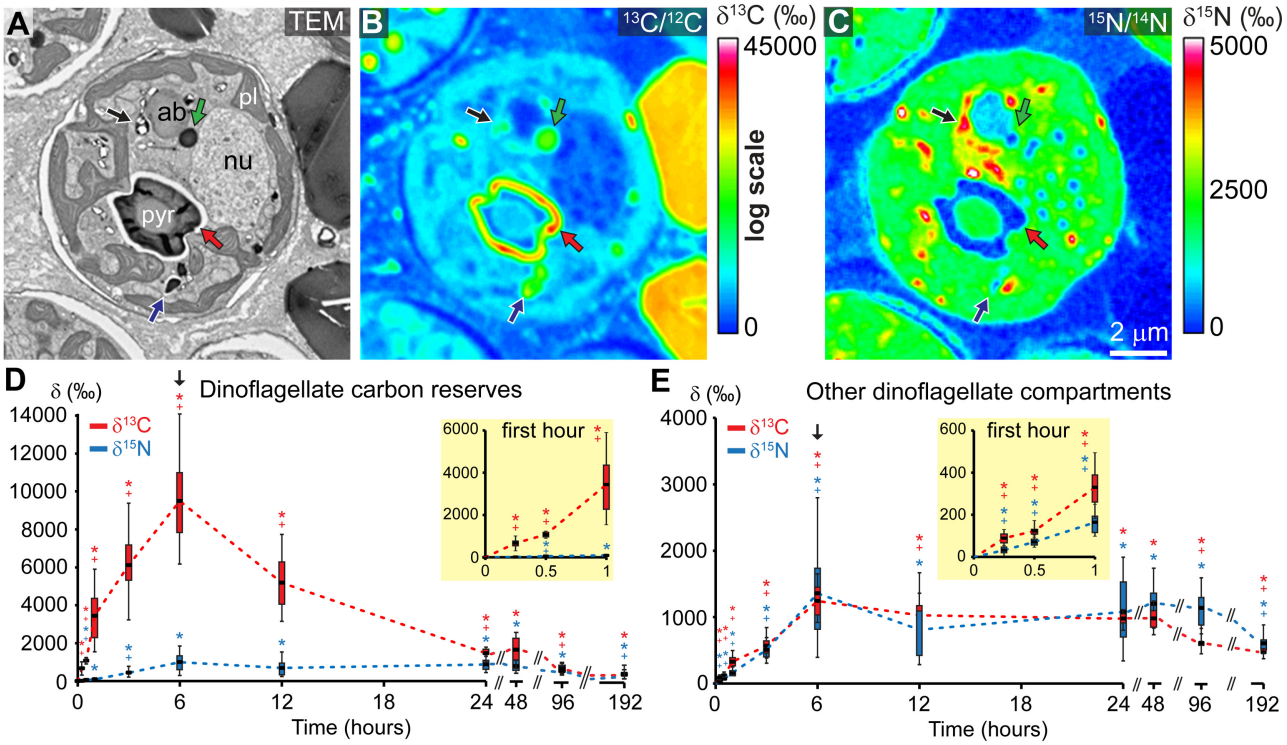

FIG 1 Photosynthesis-dependent carbon and nitrogen assimilation and turnover in dinoflagellate endosymbionts. (A) TEM micrograph of a representative dinoflagellate cell within the coral oral gastroderm after 6 h in the pulse of dual isotopic labeling under light with [^{13}C]bicarbonate (2 mM) and [^{15}N]nitrate (30 μM). (B and C) Corresponding NanoSIMS ^{13}C/^{12}C (B) and ^{15}N/^{14}N (C) isotopic images. (D and E) NanoSIMS quantified ^{13}C/^{12}C (in red) and ^{15}N/^{14}N (in blue) isotope ratios in the dinoflagellate C reserves (including lipid droplets and starch granules) and in the remaining dinoflagellate compartments, respectively, during the pulse-chase experiment conducted for 8 days under light/dark cycling (12 h/12 h). The black arrow on graphs indicates the end of the 6-h pulse of labeling under light. Significant differences (pairwise Wilcoxon rank sum test or pairwise *t* test, $P < 0.05$) are indicated between labeled and unlabeled control corals (*) and between samples from two consecutive time points (+); the number of replicate ROIs and *P* values of statistical analyses are given in Data Set S1 in the supplemental material; the box-whisker plot separates data into quartiles, with the top of the box defining the 75th percentile, the bottom the 25th percentile, the middle line the average value, the upper "whisker" the 95th percentile, and the lower "whisker" the 5th percentile. ab, accumulation body; nu, nucleus; pl, plastid; pyr, pyrenoid; red arrows, primary starch; blue arrows, secondary starch; green arrows, dinoflagellate LDs; black arrows, vesicles containing uric acid crystals.

in the coral LDs from the oral gastroderm. In contrast, incorporation into coral LDs from the three other epithelia was much less efficient and occurred with a 3-h delay (Fig. 2A, B, and E; see Data Set S1 and Fig. S6). In the 186-h chase, coral LDs from the oral gastroderm were then strongly depleted in ^{13}C, with more than a 90% decrease in average ^{13}C enrichment compared to the peak value at the end of the pulse (Fig. 2E). Note the very high level of variability in ^{13}C enrichments among individual coral LDs from the oral gastroderm, especially after 6 h in the pulse (Fig. 2E).

At the end of the 6-h pulse, ^{13}C-labeled photosynthates translocated by dinoflagellates were also systematically found associated with numerous ~50-nm-diameter glycogen granules, located in the apical region of coral cells from the oral epiderm (Fig. 3). (An enlarged view of Fig. 3D is provided in Fig. S7 in the supplemental material.) In these areas rich in glycogen granules, the ^{13}C labeling was found from NanoSIMS line profiles to gradually decrease over the 186-h chase under light/dark cycling, reaching ~85% ^{13}C depletion compared to the peak value at the end of the pulse (see Fig. S8 in the supplemental material).

Translocation by dinoflagellates of ^{15}N-labeled photosynthates to the coral tissue (overall coral cells) was recorded starting after 3 h into the pulse—i.e., with a much longer delay in comparison to ^{13}C (Fig. 2D). Moreover, in contrast to translocated ^{13}C, the spatial distribution of translocated ^{15}N was found to be relatively homogeneous in coral cells, with no specific subcellular compartments in the host tissue benefitting preferentially from the dinoflagellate supply of ^{15}N-labeled materials (Fig. 2A and C; see Fig. S6 in the supplemental material). Major spatial patterns and temporal time scales of ^{13}C and ^{15}N fluxes in the symbiosis are summarized in Table 1.

DISCUSSION

Subcellular imaging of photosynthetic C and N assimilation and utilization by the dinoflagellate endosymbionts. This study demonstrates that in the tropical reef-building coral *P. damicornis*, a substantial fraction of photosynthetically assimilated inorganic C and N was retained in the dinoflagellate cells during the pulse-chase experiments. C-containing photosynthates rapidly (within 15 min) accumulated into dinoflagellate lipid droplets (LDs) and starch granules (both primary and secondary), with subsequent rapid turnover. Most accumulated ^{13}C was depleted from dinoflagellate C reserves within the first 18 h of the chase under light/dark cycling, over a period that includes the first 12-h dark phase. This result strongly suggests a diurnal rhythmicity in the formation (under light) and utilization (under dark) of LDs and starches by dinoflagellates. The ^{15}N labeling observed in the ^{13}C-enriched di-

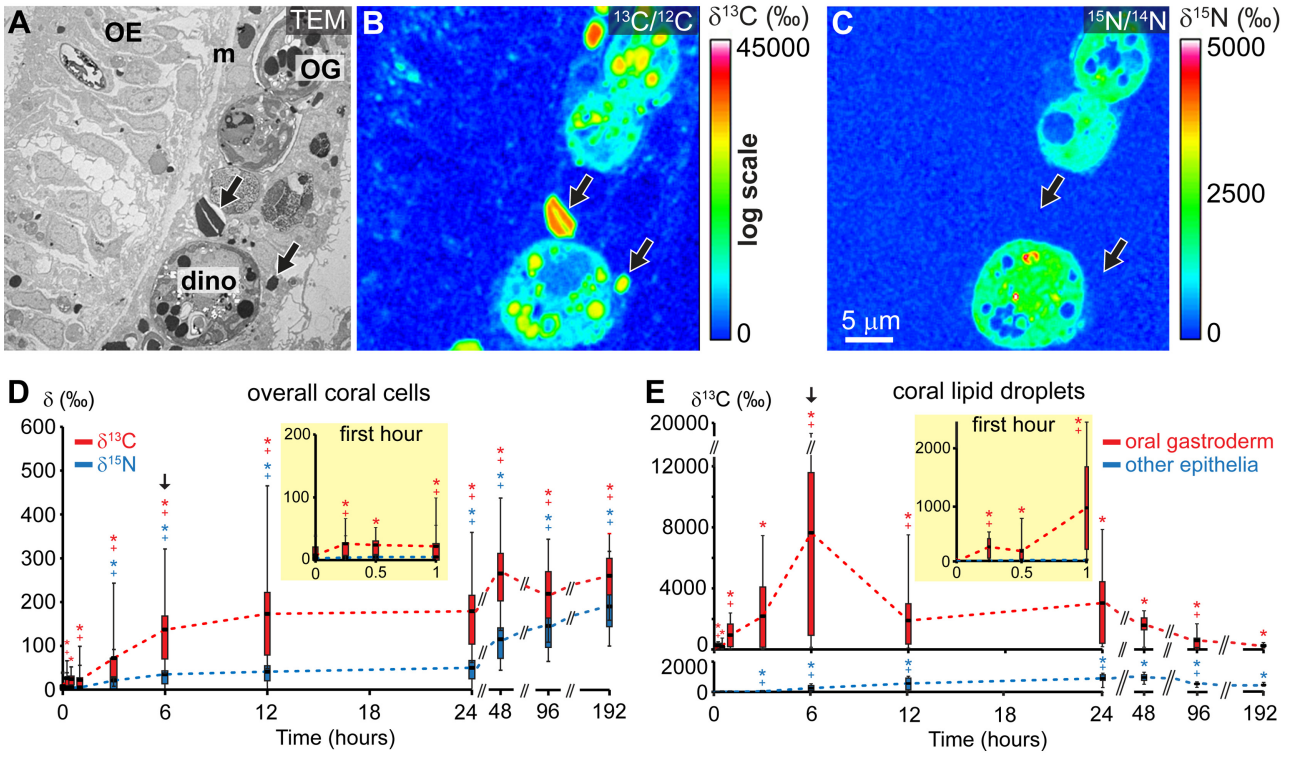

FIG 2 Photosynthate translocation from dinoflagellates into the coral host tissue and their lipid droplets. (A) Representative TEM micrograph of the coral oral tissue after 6 h in the pulse of dual isotopic labeling under light. (B and C) Corresponding NanoSIMS $^{13}C/^{12}C$ (B) and $^{15}N/^{14}N$ (C) isotopic images. (D) NanoSIMS quantified $^{13}C/^{12}C$ (in red) and $^{15}N/^{14}N$ (in blue) isotopic ratios in the whole coral tissue (including all four epithelia) during the pulse-chase experiment under light/dark cycling. (E) NanoSIMS quantified $^{13}C/^{12}C$ isotopic ratio in coral lipid droplets from the oral gastroderm (in red) and from the three other epithelia (oral epiderm, aboral gastroderm, and calicoderm [in blue]). Results and their statistical significance are reported as described in the legend to Fig. 1. OE, oral epiderm; OG, oral gastroderm; m, mesoglea; dino, dinoflagellate cell; black arrows, coral lipid droplets.

noflagellate LDs and starch granules most likely reflects the incorporation of ^{15}N-labeled proteins, possibly enzymes involved in the synthesis and further catabolism of neutral lipids or carbohydrates, onto the surface or into the internal matrix of these compartments (35, 36). In addition, assimilated ^{13}C and ^{15}N were allocated to the various other dinoflagellate compartments (including, e.g., the nucleus and plastid), albeit for C with a lower efficiency and a slower turnover than for the C reserves, most likely reflecting the utilization of C and N for dinoflagellate maintenance, growth, and division.

These NanoSIMS results obtained *in situ* (i.e., in the intact coral-dinoflagellate association) are in agreement with data from previous bulk-level isotopic incubation analyses with ^{14}C- or ^{13}C-labeled bicarbonate, which report a rapid loss of ^{14}C or ^{13}C enrichment in the dinoflagellate fraction within the first hours of the chase, especially during the first night (17, 21, 37–39). In particular, by labeling the reef coral *Acropora pulchra* simultaneously with [^{13}C]bicarbonate and [^{15}N]nitrate, Tanaka et al. (21) found a dramatic nighttime decrease in the dinoflagellate fraction of the C:N ratio of light-produced compounds, suggesting rapid consumption of photosynthates with high C content (i.e., lipids and carbohydrates) by dinoflagellate respiration. Conversely, in *Stylophora pistillata* colonies, the rapid decrease in ^{14}C or ^{13}C labeling of the dinoflagellate fraction, observed over a chase period of 24 to 48 h, was mainly ascribed to delayed translocation of ^{14}C- or ^{13}C-labeled photosynthates to the coral host partner (17, 39).

Here, we observed that the rapid ^{13}C decrease in dinoflagellate endosymbionts of *P. damicornis* is occurring via isotopic depletion of their intracellular LDs and starch granules and not through depletion of their other cell compartments. This result supports the hypothesis that lipids and carbohydrates stored by dinoflagellates during daytime are quickly remobilized, especially during nighttime, via mitochondrial respiration (releasing $^{13}CO_2$) to sustain dinoflagellate metabolism. Nevertheless, the following additional mechanisms for such rapid ^{13}C depletion in dinoflagellate C reserves cannot be excluded: (i) the effect of an isotopic dilution due to the additional storage of newly produced [^{12}C]photosynthates during the light periods of the chase, (ii) the translocation of ^{13}C-labeled compounds toward the coral host tissue (during light and dark periods of the chase), and/or (iii) the remobilization of stored ^{13}C as building blocks for dinoflagellate maintenance, growth, and division.

Interestingly, by maintaining *P. damicornis* microcolonies under constant darkness, a treatment known to trigger coral bleaching after about 4 days (40, 41), the ultrastructural disappearance of dinoflagellate LDs and starch granules was systematically accompanied by features of cell vacuolization and damage of organelles, indicative of *in situ* degradation of the endosymbionts. These observations are additional evidence that photosynthates stored in dinoflagellates under light are essential to further sustain their respiration and metabolism, especially during nighttime.

In marine microalgae, photosynthates produced and stored

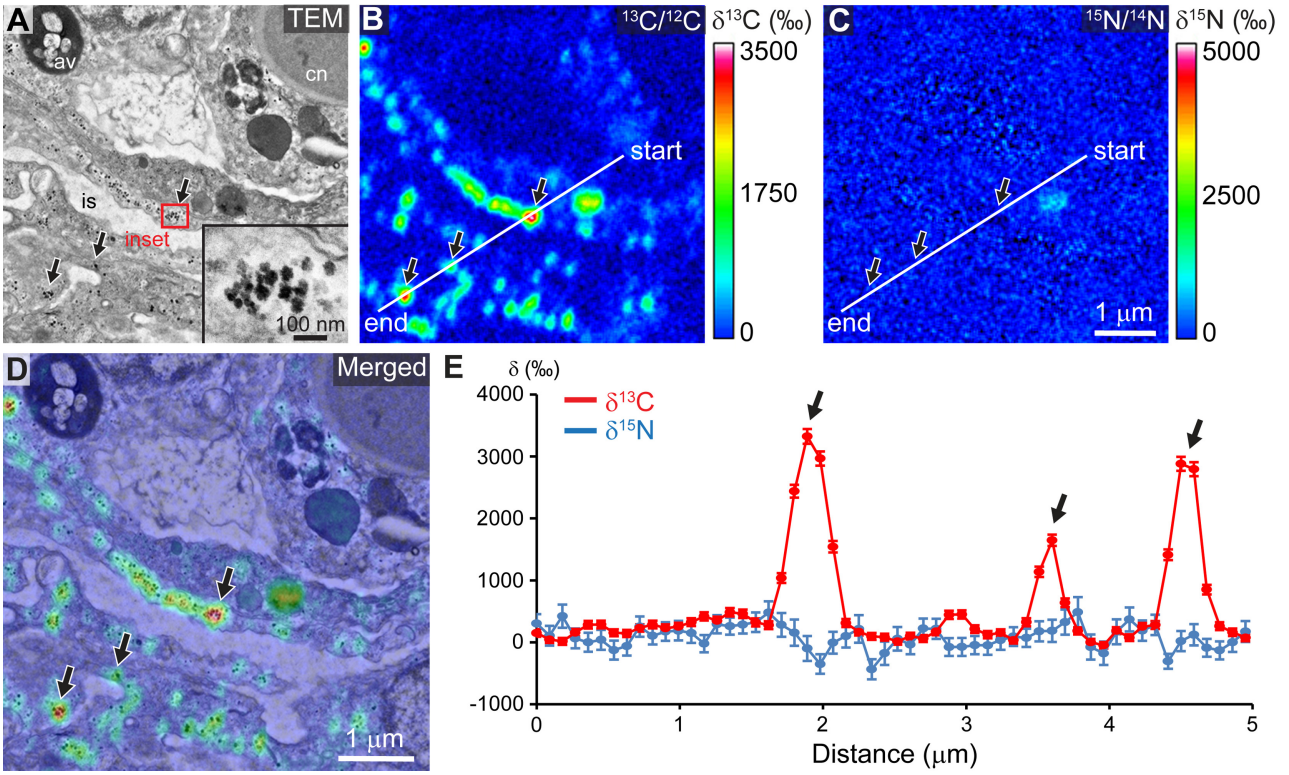

FIG 3 Photosynthate accumulation into coral glycogen granules. (A) Representative TEM micrograph of the coral oral epiderm with a higher-magnification view of glycogen granules (inset). (B and C) Corresponding NanoSIMS $^{13}C/^{12}C$ (B) and $^{15}N/^{14}N$ (C) isotopic images. (D) Merged image between the TEM micrograph and the NanoSIMS $^{13}C/^{12}C$ isotopic map. An enlarged view is provided in Fig. S7 in the supplemental material. (E) Fluctuations of both ^{13}C (in red) and ^{15}N (in blue) enrichments along the NanoSIMS profile depicted in panels B and C. Standard deviations of the mean are based on Poisson statistics. Black arrows point to areas rich in glycogen granules. av, autophagic vacuole; cn, cnidocyte; is, intercellular space.

under light might provide C skeletons and energy to support DIN (ammonium and nitrate) uptake and assimilation in the dark (42). The existence of an internal C reservoir in dinoflagellate endosymbionts, metabolized during nighttime to sustain N acquisition, is suggested by the extended time of darkness (at least 15 h) needed to efficiently inhibit ammonium incorporation in symbiotic reef corals (5, 33). Similarly, we demonstrate that prolonged dark pretreatment (24 h) fully repressed nitrate assimilation in dinoflagellates of the reef coral *P. damicornis*. Interestingly, in coastal marine environments, migrating free-living dinoflagellates reach the illuminated sea surface, poor in DIN, during the day, to accumulate excess photosynthates not channeled toward protein synthesis, whereas they descend during the night to a depth enriched in nitrate, which is then efficiently assimilated through the remobilization of light-produced C reserves (43). Hence, the storage of lipids and carbohydrates by dinoflagellates during daytime might constitute a C reserve helping reef corals to efficiently sustain DIN acquisition during nighttime, representing an adaption to nutrient-poor environments.

The fate of C and N translocated to the coral host. The present study reveals the subcellular pathways of photosynthetic C translocation from the dinoflagellate cells toward all four epithelia composing the coral host tissue, extending our previous NanoSIMS observations of transepithelial movements of nitrogenous compounds translocated by the endosymbionts (32, 33). In early autoradiographic investigations, transepithelial metabolite fluxes

TABLE 1 Summary of the main events and time scales traced in this study

Symbiotic partner	Major event traced	Time scale
Dinoflagellates	Photosynthesis-dependent assimilation of bicarbonate and nitrate	15 min
	C allocation to C reserves (lipid droplets and starch)	15 min
	C turnover in C reserves related to diurnal light cycle	~80% ^{13}C depletion in 18 h
	C and N turnover in other compartments	~60% ^{13}C and ^{15}N depletion in 186 h
Coral	C translocation by dinoflagellates	15 min
	N translocation by dinoflagellates	3 h
	Allocation of translocated C to lipid droplets (oral gastroderm)	15 min
	Allocation of translocated C to glycogen (oral epiderm)	6 h
	C turnover in lipid droplets (oral gastroderm)	>90% ^{13}C depletion in 186 h
	C turnover in glycogen (oral epiderm)	~85% ^{13}C depletion in 186 h

have been reported in marine cnidarian tissue, albeit at light microscopy level in thick histological sections (44, 45). Moreover, using bulk-level isotopic measurements of separated fractions of dinoflagellate-containing oral gastroderm and dinoflagellate-free oral epiderm prepared from tentacles of a sea anemone, Trench (18) previously found that 18 to 31% of total net photosynthates moved toward the oral epiderm within 10 h of labeling in light with [^{14}C]bicarbonate.

Here, we observed that coral LDs from the oral gastroderm epithelium constitute a major accumulation site for translocated photosynthetic ^{13}C, providing direct validation of previous hypotheses (12, 13, 15, 22, 23). The rapid C translocation toward gastrodermal coral LDs, which we visualized already at 15 min from the onset of the pulse, is consistent with results from bulk-level isotopic investigations of symbiotic sea anemones, which reported rapid translocation of photosynthates to the host fraction, within a few minutes following their production (9, 46, 47). Interestingly, we frequently observed ^{13}C-enriched LD-like structures located in the symbiosomal space between the dinoflagellate endosymbiont and the coral gastrodermal host cell (white arrows in Fig. S3 in the supplemental material). These structures have previously been interpreted as "extra-algal" LDs produced by dinoflagellates, in the process of exocytosis toward the host gastrodermal cells (48, 49). However, ultrastructural evidence for such a potential exocytotic process is still lacking. Moreover, the occurrence of LDs within coral cells of dinoflagellate-free epithelia (oral epiderm and calicoderm) implies the existence of other, still unknown, mechanisms of coral LD formation.

This study also provides evidence that coral glycogen granules in the coral oral tissue constitute another major sink for ^{13}C-photosynthates translocated by dinoflagellates. In bulk isotopic analyses of sea anemones, glucose was found to be a major metabolite translocated within minutes from the dinoflagellate endosymbionts to the host fraction (7–9). Moreover, transcriptome analyses have revealed that scleractinian (*Acropora* genus) corals have the enzymatic machinery for synthesis and remobilization of glycogen from and to glucose (26). Consistent with these reports, combined TEM and NanoSIMS observations show incorporation (within 6 h) of external [$^{13}C_6$]glucose (30 μM) into glycogen granules of the coral oral epidermal cells (see Fig. S9 in the supplemental material). Thus, our results provide direct evidence of the functional mechanisms of storage of photosynthetic C, translocated by the dinoflagellate endosymbionts (probably in the form of glucose) to coral glycogen in the oral tissue.

Similar to dinoflagellate C reserves, the ^{13}C depletion observed for coral LDs in the oral gastroderm and for the glycogen granules in the oral tissue most likely reflects the breakdown of neutral lipids and carbohydrates to sustain coral cell respiration. Nevertheless, we cannot exclude the potential contribution of (i) an isotopic dilution effect resulting from the translocation of photosynthates with normal C isotopic composition to coral LDs and glycogen and (ii) the reallocation of stored C toward coral cell maintenance, growth, and division.

Translocation of N-containing compounds by dinoflagellates was not recorded immediately in the coral host partner but was observed with a delay of 3 h following the onset of the pulse-chase experiment under light/dark cycling, confirming previous observations (33). These results suggest a temporal separation between the translocation by dinoflagellates of C- and N-containing photosynthetic assimilates. Compounds bearing C are released within a few minutes after their production, compared to a time scale of hours for N-bearing compounds (summarized in Table 1). It is also possible that early translocation of N to the coral tissue has been partly masked by a potentially high rate of N recycling by the dinoflagellates (5) or by extraction of low-molecular-weight soluble nitrogenous compounds (e.g., free amino acids) during sample preparation. Alternative NanoSIMS sample preparation methods (e.g., cryofixation and cryosubstitution) might improve tracking of low-molecular-weight soluble photosynthates.

Conclusion. By combining pulse-chase double stable-isotopic labeling (^{13}C and ^{15}N) with TEM ultrastructural and NanoSIMS isotopic imaging, we have visualized and quantified at subcellular levels the incorporation and turnover of C and N in the symbiotic reef-building coral *P. damicornis*. These results provide a qualitative baseline of subcellular allocation and turnover of C- and N-containing photosynthates in the coral-dinoflagellate symbiosis. In the future, more precise quantitative C and N budgets for symbiotic reef corals could be constructed, using additional respiration and photosynthesis measurements. Moreover, alterations in the pattern of C and N utilization by symbiotic corals might be more precisely characterized in response to heterotrophic feeding and to global environmental changes.

MATERIALS AND METHODS

Design of ^{13}C and ^{15}N dual isotopic labeling experiments. Experiments were carried out on microcolonies (~5 cm tall) of the reef-building coral *Pocillopora damicornis* (Linnaeus, 1758) prepared from one large colony grown at the Aquarium Tropical, Palais de la Porte Dorée, Paris, France. Coral microcolonies were acclimatized for 4 weeks prior to experimental manipulation in a large tank equilibrated with fish and benthic organisms, filled with artificial seawater (Instant Ocean Salts) and containing low nutrient concentrations (NH_4^+, <1 μM; NO_2^-, <1 μM; NO_3^- <5 μM; PO_4^{3-}, <1 μM [Salifert tests]). The temperature was 25 $\pm$ 1°C, the salinity was 35 $\pm$ 1‰, and the pH was 8.1 $\pm$ 0.1. Light irradiance of 100 μmol $\cdot$ m^{-2} $\cdot$ s^{-1} in the photosynthetically active radiation range was provided by 8 fluorescent T5 tubes of 39 W (6 $\times$ 10,000 K, 2 $\times$ 20,000 K) with 12-h/12-h light/dark cycling. During the acclimatization period of 4 weeks and subsequent experiments, coral microcolonies were not fed with plankton and therefore mostly relied on the uptake and assimilation of particulate and dissolved organic matter and on the autotrophic input from their photosynthetic dinoflagellate symbionts.

Isotopic dual labeling pulse-chase experiments were conducted in closed-system 20-liter glass tanks. In a first step, 17 coral microcolonies were incubated for 6 h in light in 0.2-μm-pore-filtered artificial seawater (adapted from Harrison et al. [50]), initially free of bicarbonate and nitrate, and supplemented with 2 mM [^{13}C]bicarbonate ($NaH^{13}CO_3$, 99 atom% [Sigma-Aldrich]) and 30 μM [^{15}N]nitrate ($K^{15}NO_3$, 98 atom% [Sigma-Aldrich]). This pulse of isotopic dual labeling started about 2 h after the onset of the light period. Then 5 coral microcolonies were transferred for a 186-h (8-day) chase period with light/dark cycling (12 h/12 h) in a tank filled with 20 liters artificial seawater sampled from the large acclimatization tank with normal C and N isotopic composition. The effect of coral autotrophic starvation on C and N remobilization pattern was investigated in a parallel 186-h chase experiment with 5 coral microcolonies exposed to similar conditions but maintained under constant darkness. During the chase phase, 25% of the incubation volume was renewed daily with artificial seawater from the large acclimatization tank. For TEM ultrastructural and NanoSIMS isotopic imaging, apexes of coral branches were sampled with cutting pliers during the pulse-chase experiments at 0, 0.25, 0.5, 1, 3, 6, 12, 24, 48, 96, and 192 h, respectively. At each time step, a different coral microcolony (nubbin) was sampled, except at 6 h, where 3 replicate nubbins were sampled. Throughout the pulse-chase experiment under light/dark cycling, coral microcolonies displayed no

macromorphological indications of stress (i.e., no unusual tentacle retraction, extensive mucus secretion, or paling). During the chase period, ammonium and nitrate concentrations fluctuated mildly between values of 1 to 4 μM and 5 to 10 μM, respectively, corresponding to closed-system aquarium conditions.

Contribution of nonphotosynthetic carboxylation reactions ("heterotrophic" C fixation) to [^{13}C]bicarbonate incorporation by the symbiotic system and the effect of dark inhibition on [^{15}N]nitrate assimilation by symbiotic dinoflagellates were assessed as follows: 3 coral microcolonies were pretreated for 24 h under constant darkness and then incubated for 6 h in darkness in a tank filled with 2 liters of 0.2-μm-pore-filtered artificial seawater (adapted from Harrison et al. [50]), initially free of bicarbonate and nitrate and supplemented with 2 mM [^{13}C]bicarbonate ($NaH^{13}CO_3$, 99 atom% [Sigma-Aldrich]) and 30 μM [^{15}N]nitrate ($K^{15}NO_3$, 98 atom% [Sigma-Aldrich]). Such extended pretreatment under darkness is required to effectively inhibit DIN assimilation in symbiotic reef corals (5, 33). Apexes of coral branches were sampled with cutting pliers at 0, 3, and 6 h during the labeling pulse.

To limit spatial fluctuations due to metabolic heterogeneities along coral branches or between different coral tissue areas (51–53), TEM ultrastructural observations and NanoSIMS isotopic quantitative imaging were systematically performed on coral tissue sampled from the subapical area of light-exposed branches, within the coenosarcal connective tissue linking polyp units together (see Fig. S1 in the supplemental material)

TEM ultrastructural observations. Coral samples were chemically fixed for 24 h at room temperature in Sörensen-sucrose phosphate buffer (0.1 M phosphate at pH 7.5, 0.6 M sucrose, 1 mM $CaCl_2$) containing both 2.5% glutaraldehyde and 1% formaldehyde. They were then decalcified for 4 to 5 days in 0.1 M Sörensen phosphate buffer containing 0.5 M EDTA at 4°C. Tissue samples were dissected under the stereomicroscope into small pieces containing one or two polyps, postfixed 1 h at room temperature with 1% OsO_4 in 0.1 M Sörensen phosphate buffer, dehydrated in graded series of ethanol (50, 70, 90, and 100%), and embedded in Spurr's resin. Tissue was preferentially oriented to obtain longitudinal sections parallel to the vertical growth direction of polyps. Sections were cut with a Diatome 45° diamond knife. Semithin sections (~0.5 μm) were stained with methylene blue-Azur II and observed with a Zeiss Axio Imager Z2 light microscope equipped with a Zeiss AxioCamMRc 5 digital camera. Ultrathin sections (~70 to 90 nm) were mounted on Formvar carbon-coated alphanumeric grids counterstained with 4% uranyl acetate and Reynold's lead citrate solution. Ultrastructural observations were carried out at 80 kV with a Philips CM 100 transmission electron microscope within the Electron Microscopy Facility (EMF) at the University of Lausanne (Switzerland).

Quantitative NanoSIMS isotopic imaging and ROI definition. In order to image and quantify *in situ* the subcellular distribution of ^{13}C and ^{15}N enrichment within endosymbiotic dinoflagellate cells and coral host tissue, the exact same areas in the coral tissue imaged by TEM were analyzed with the NanoSIMS 50L ion microprobe in the Laboratory for Biological Geochemistry (EPFL, Lausanne, Switzerland), enabling direct correlation of ultrastructural (TEM) and isotopic (NanoSIMS) images.

TEM grids were mounted on 10-mm aluminum stubs with double-stick Cu tape and coated with about a 10-nm thickness of gold. They were bombarded with a 16-keV primary ion beam of Cs^+ (1 to 3 pA) focused to a spot size of about 100 to 150 nm on the sample surface. Secondary molecular ions $^{12}C_2^-$, $^{13}C^{12}C^-$, $^{12}C^{14}N^-$, and $^{12}C^{15}N^-$ were simultaneously collected in electron multipliers at a mass resolution sufficient to avoid potentially problematic isobaric interferences on $^{13}C^{12}C^-$ and $^{12}C^{15}N^-$. Charge compensation was not necessary. Isotopic images ranging between 5 × 5 μm^2 and 50 × 50 μm^2 with 256 by 256 pixels were obtained by rastering the primary beam across the sample surface with a dwell time of 5 ms. ^{13}C/^{12}C and ^{15}N/^{14}N ratio distribution maps were obtained by taking the ratio between the drift-corrected $^{13}C^{12}C^-$ and $^{12}C_2^-$ images and $^{12}C^{15}N^-$ and $^{12}C^{14}N^-$ images, respectively. ^{13}C and ^{15}N enrichments were expressed in the following delta notations:

$$\delta^{13}C\ (\text{‰}) = \left(\frac{C_{mes}}{C_{nat}} - 1\right) \times 1,000 \quad (1)$$

where C_{mes} is the measured ^{13}C/^{12}C ratio and C_{nat} is the average natural ^{13}C/^{12}C ratio measured several times per day in nonlabeled, identically prepared coral samples throughout the period of NanoSIMS analyses and

$$\delta^{15}N\ (\text{‰}) = \left(\frac{N_{mes}}{N_{nat}} - 1\right) \times 1,000 \quad (2)$$

where N_{mes} is the measured ^{15}N/^{14}N ratio and N_{nat} is the average natural ^{15}N/^{14}N ratio measured several times per day in nonlabeled, identically prepared coral samples throughout the period of NanoSIMS analyses.

For each ultrathin section analyzed (for each coral microcolony sampled at each time step of the pulse-chase experiments), ~12 NanoSIMS isotopic maps were acquired to obtain a representative view of both isotopic enrichment and spatial distribution within the coral-dinoflagellate system. All analyzed dinoflagellates in this study were located in the oral gastroderm epithelium, which contains by far the highest density of symbiotic cells compared to the aboral gastroderm (see Fig. S1 in the supplemental material).

Data were processed using the L'IMAGE software. A smooth width of 3 pixels was applied for NanoSIMS ^{13}C/^{12}C and ^{15}N/^{14}N isotopic images, and a line width of 1 pixel was applied when illustrative line scans were defined from these smoothed images. NanoSIMS quantification of both ^{13}C and ^{15}N enrichments was carried out by defining regions of interest (ROIs), as illustrated in Fig. S2 in the supplemental material. For the whole dinoflagellates and their C reserves (i.e., starch granules and LDs), the ROIs were obtained by drawing their contours. Quantification of the remaining cell compartments (i.e., the whole dinoflagellate cell minus the C reserves) was obtained by subtracting corresponding ROIs. In the coral host tissue, ROIs were defined as circles of 2 to 3 μm covering each of the four coral epithelia, avoiding the mesoglea and intercellular spaces. For coral LDs, ROIs were obtained by drawing their contours. Because their small size (~50 nm in diameter) prevented accurate drawing of ROIs around each glycogen granule, their accumulation and turnover were assessed qualitatively from NanoSIMS line scans, and the spatial correlation between isotopic labeling and glycogen granules was confirmed in merged TEM and NanoSIMS images.

Importantly, conventional TEM sample preparation (i.e., chemical fixation with aldehydes and osmium tetroxide postfixation, followed by decalcification and ethanol dehydration) extracts most low-molecular-weight soluble compounds and diffusible ions located in coral and dinoflagellate cells. Consequently, we imaged with NanoSIMS ^{13}C and ^{15}N incorporation into macromolecules (e.g., proteins, unsaturated lipids, and carbohydrates, such as glycogen and starch) stabilized by the sample preparation procedure.

Statistical analyses. Data were statistically analyzed with the R software. Shapiro-Wilk and Bartlett tests were used to assess data normality and homoscedasticity. In the case of non-Gaussian distributions, the nonparametric Kruskal-Wallis test was applied combined with a pairwise Wilcoxon rank sum test, instead of the one-way analysis of variance (ANOVA) combined with a pairwise *t* test. Holm's correction was systematically employed when doing pairwise multiple-comparison tests. Results were considered significant at the 5% level.

SUPPLEMENTAL MATERIAL

Supplemental material for this article may be found at http://mbio.asm.org/lookup/suppl/doi:10.1128/mBio.02299-14/-/DCSupplemental.

Figure S1, JPG file, 0.5 MB.
Figure S2, JPG file, 1.9 MB.
Figure S3, JPG file, 2.2 MB.
Figure S4, JPG file, 1.7 MB.
Figure S5, JPG file, 1.2 MB.
Figure S6, JPG file, 2.2 MB.
Figure S7, JPG file, 1.8 MB.
Figure S8, JPG file, 2.1 MB.

Figure S9, JPG file, 2.3 MB.
Data Set S1, XLSX file, 0.03 MB.

ACKNOWLEDGMENTS

This work was supported by European Research Council advanced grant 246749 (BIOCARB), Fonds National Suisse grant CR2312-141048, and the École Polytechnique Fédérale de Lausanne to A.M., CNRS grant Interface 2010 (NanoSIMS and symbiosis) to I.D.C., and the Faculty of Biology and Medicine of the University of Lausanne.

We thank Jean Daraspe, Chakib Djediat, Céline Loussert, and Antonio Mucciolo for providing help with TEM preparations. We are grateful for access to and expert help with aquarium facilities at ATPD, in particular to Jean-Daniel Galois and Sylvain Joumier. Mathieu Pernice, Stephanie Cohen, and Thomas Krueger are thanked for discussions. Two anonymous reviewers are thanked for highly constructive comments and suggestions that helped improve the manuscript.

REFERENCES

1. **Venn AA, Loram JE, Douglas AE.** 2008. Photosynthetic symbioses in animals. J Exp Bot **59:**1069–1080. http://dx.doi.org/10.1093/jxb/erm328.
2. **Yellowlees D, Rees TA, Leggat W.** 2008. Metabolic interactions between algal symbionts and invertebrate hosts. Plant Cell Environ **31:**679–694. http://dx.doi.org/10.1111/j.1365-3040.2008.01802.x.
3. **Davy SK, Allemand D, Weis VM.** 2012. Cell biology of cnidarian-dinoflagellate symbiosis. Microbiol Mol Biol Rev **76:**229–261. http://dx.doi.org/10.1128/MMBR.05014-11.
4. **Trench R.** 1993. Microalgal-invertebrate symbioses—a review. Resources **9:**135–175.
5. **Muscatine L, D'Elia CF.** 1978. The uptake, retention, and release of ammonium by reef corals. Limnol Oceangr **23:**725–734. http://dx.doi.org/10.4319/lo.1978.23.4.0725.
6. **Rahav O, Dubinsky Z, Achituv Y, Falkowski PG.** 1989. Ammonium metabolism in the zooxanthellate coral, *Stylophora pistillata*. Proc R Soc Lond B Biol Sci **236:**325–337. http://dx.doi.org/10.1098/rspb.1989.0026.
7. **Muscatine L, Cernichiari E.** 1969. Assimilation of photosynthetic products of zooxanthellae by a reef coral. Biol Bull **137:**506–523. http://dx.doi.org/10.2307/1540172.
8. **Whitehead LF, Douglas AE.** 2003. Metabolite comparisons and the identity of nutrients translocated from symbiotic algae to an animal host. J Exp Biol **206:**3149–3157. http://dx.doi.org/10.1242/jeb.00539.
9. **Burriesci MS, Raab TK, Pringle JR.** 2012. Evidence that glucose is the major transferred metabolite in dinoflagellate-cnidarian symbiosis. J Exp Biol **215:**3467–3477. http://dx.doi.org/10.1242/jeb.070946.
10. **Papina M, Meziane T, Van Woesik R.** 2003. Symbiotic zooxanthellae provide the host-coral *Montipora digitata* with polyunsaturated fatty acids. Comp Biochem Physiol B Biochem Mol Biol **135:**533–537. http://dx.doi.org/10.1016/S1096-4959(03)00118-0.
11. **Markell DA, Trench RK.** 1993. Macromolecules exuded by symbiotic dinoflagellates in culture: amino acid and sugar composition. J Phycol **29:**64–68. http://dx.doi.org/10.1111/j.1529-8817.1993.tb00280.x.
12. **Patton JS, Abraham S, Benson AA.** 1977. Lipogenesis in the intact coral *Pocillopora capitata* and its isolated zooxanthellae: evidence for a light-driven carbon cycle between symbiont and host. Mar Biol **44:**235–247. http://dx.doi.org/10.1007/BF00387705.
13. **Stimson JS.** 1987. Location, quantity and rate of change in quantity of lipids in tissue of Hawaiian hermatypic corals. Bull Mar Sci **41:**889–904.
14. **Harland AD, Navarro JC, Spencer Davies P, Fixter LM.** 1993. Lipids of some Caribbean and Red Sea corals: total lipid, wax esters, triglycerides and fatty acids. Mar Biol **117:**113–117. http://dx.doi.org/10.1007/BF00346432.
15. **Peng SE, Chen WN, Chen HK, Lu CY, Mayfield AB, Fang LS, Chen CS.** 2011. Lipid bodies in coral-dinoflagellate endosymbiosis: proteomic and ultrastructural studies. Proteomics **11:**3540–3555. http://dx.doi.org/10.1002/pmic.201000552.
16. **Von Holt C, Von Holt M.** 1968. Transfer of photosynthetic products from zooxanthellae to coelenterate hosts. Comp Biochem Physiol **24:**73–81. http://dx.doi.org/10.1016/0010-406X(68)90959-6.
17. **Muscatine L, Falkowski PG, Porter JW, Dubinsky Z.** 1984. Fate of photosynthetic fixed carbon in light- and shade-adapted colonies of the symbiotic coral *Stylophora pistillata*. Proc R Soc Lond B Biol Sci **222:**181–202. http://dx.doi.org/10.1098/rspb.1984.0058.
18. **Trench R.** 1971. The physiology and biochemistry of zooxanthellae symbiotic with marine coelenterates. I. The assimilation of photosynthetic products of zooxanthellae by two marine coelenterates. Proc R Soc Lond B Biol Sci **177:**225–235.
19. **Cooksey KE, Cooksey B.** 1972. Turnover of photosynthetically fixed carbon in reef corals. Mar Biol **15:**289–292. http://dx.doi.org/10.1007/BF00401387.
20. **Crossland CJ, Barnes DJ, Cox T, Devereux M.** 1980. Compartmentation and turnover of organic carbon in the staghorn coral *Acropora formosa*. Mar Biol **59:**181–187. http://dx.doi.org/10.1007/BF00396866.
21. **Tanaka Y, Miyajima T, Koike I, Hayashibara T, Ogawa H.** 2006. Translocation and conservation of organic nitrogen within the coral-zooxanthella symbiotic system of *Acropora pulchra*, as demonstrated by dual isotope-labeling techniques. J Exp Mar Biol Ecol **336:**110–119. http://dx.doi.org/10.1016/j.jembe.2006.04.011.
22. **Luo Y-J, Wang L-H, Chen W-NU, Peng S-E, Tzen JT-C, Hsiao Y-Y, Huang H-J, Fang L-S, Chen C-S.** 2009. Ratiometric imaging of gastrodermal lipid bodies in coral-dinoflagellate endosymbiosis. Coral Reefs **28:**289–301. http://dx.doi.org/10.1007/s00338-008-0462-8.
23. **Chen W-NU, Kang H-J, Weis VM, Mayfield AB, Jiang P-L, Fang L-S, Chen C-S.** 2012. Diel rhythmicity of lipid-body formation in a coral-Symbiodinium endosymbiosis. Coral Reefs **31:**521–534. http://dx.doi.org/10.1007/s00338-011-0868-6.
24. **Hosoi K.** 1938. Contribution to the biochemistry of the coral. 1. On the occurrence of glycogen and its content in the polyp of Fungia actiniformis var. palawensis Döderlein Palao. Trop Biol Stn **3:**447–451.
25. **Hayes RL, Goreau NI.** 1977. Intracellular crystal-bearing vesicles in the epidermis of scleractinian corals, *Astrangia danae* (Agassiz) and *Porites porites* (Pallas). Biol Bull **152:**26–40. http://dx.doi.org/10.2307/1540724.
26. **Leggat W, Seneca F, Wasmund K, Ukani L, Yellowlees D, Ainsworth TD.** 2011. Differential responses of the coral host and their algal symbiont to thermal stress. PLoS One **6**(10):e26687. http://dx.doi.org/10.1371/journal.pone.0026687.
27. **Doyle WL, Doyle MM.** 1940. The structure of zooxanthellae. Tortugas Lab **32:**129–142.
28. **Taylor DL.** 1968. In situ studies on the cytochemistry and ultrastructure of a symbiotic marine dinoflagellate. J Mar Biol Assoc **48:**349–366. http://dx.doi.org/10.1017/S0025315400034548.
29. **Lechene, Francois H, Douglas B, Patrick KJ, Daniel D, Yvette L, Joseph B, Kwon P, Susumu I, Gilles B, Park KM, Ito S, Schwartz M, Benichou G, Slodzian G.** 2006. High-resolution quantitative imaging of mammalian and bacterial cells using stable isotope mass spectrometry. J Biol **5:**20. http://dx.doi.org/10.1186/jbiol42.
30. **Clode PL, Stern RA, Marshall AT.** 2007. Subcellular imaging of isotopically labeled carbon compounds in a biological sample by ion microprobe (NanoSIMS). Microsc Res Tech **70:**220–229. http://dx.doi.org/10.1002/jemt.20409.
31. **Hoppe P, Cohen S, Meibom A.** 2013. NanoSIMS: technical aspects and applications in cosmochemistry and biological geochemistry. Geostand Geoanal Res **37:**111–154. http://dx.doi.org/10.1111/j.1751-908X.2013.00239.x.
32. **Pernice M, Meibom A, Van Den Heuvel A, Kopp C, Domart-Coulon I, Hoegh-Guldberg O, Dove S, Wang D, Huang R, Chang X, Chain PS, Xie G, Ling J, Xu J.** 2012. A single-cell view of ammonium assimilation in coral-dinoflagellate symbiosis. ISME J **6:**1314–1324. http://dx.doi.org/10.1038/ismej.2011.196.
33. **Kopp C, Pernice M, Domart-Coulon I, Djediat C, Spangenberg JE, Alexander DT, Hignette M, Meziane T, Meibom A.** 2013. Highly dynamic cellular-level response of symbiotic coral to a sudden increase in environmental nitrogen. mBio **4**(3):e00052-13. http://dx.doi.org/10.1128/mBio.00052-13.
34. **Clode PL, Saunders M, Maker G, Ludwig M, Atkins CA.** 2009. Uric acid deposits in symbiotic marine algae. Plant Cell Environ **32:**170–177. http://dx.doi.org/10.1111/j.1365-3040.2008.01909.x.
35. **Walther TC, Farese RV.** 2012. Lipid droplets and cellular lipid metabolism. Annu Rev Biochem **81:**687–714. http://dx.doi.org/10.1146/annurev-biochem-061009-102430.
36. **Baldwin PM.** 2001. Starch granule-associated proteins and polypeptides: a review. Starch **53:**475–503. http://dx.doi.org/10.1002/1521-379X(200110)53:10<475::AID-STAR475>3.0.CO;2-E.
37. **Patton JS, Battey JF, Rigler MW, Porter JW, Black CC, Burris JE.** 1983. A comparison of the metabolism of bicarbonate ^{14}C and acetate 1-^{14}C and

the variability of species lipid compositions in reef corals. Mar Biol 75: 121–130. http://dx.doi.org/10.1007/BF00405994.
38. **Hughes A, Grottoli A, Pease T, Matsui Y.** 2010. Acquisition and assimilation of carbon in non-bleached and bleached corals. Mar Ecol Prog Ser **420:**91–101. http://dx.doi.org/10.3354/meps08866.
39. **Tremblay P, Grover R, Maguer JF, Legendre L, Ferrier-Pagès C.** 2012. Autotrophic carbon budget in coral tissue: a new ^{13}C-based model of photosynthate translocation. J Exp Biol 215:1384–1393. http://dx.doi.org/10.1242/jeb.065201.
40. **Downs CA, Kramarsky-Winter E, Martinez J, Kushmaro A, Woodley CM, Loya Y, Ostrander GK.** 2009. Symbiophagy as a cellular mechanism for coral bleaching. Autophagy **5:**211–216. http://dx.doi.org/10.4161/auto.5.2.7405.
41. **DeSalvo MK, Estrada A, Sunagawa S, Medina M.** 2012. Transcriptomic responses to darkness stress point to common coral bleaching mechanisms. Coral Reefs **31:**215–228. http://dx.doi.org/10.1007/s00338-011-0833-4.
42. **Huppe HC, Turpin DH.** 1994. Integration of carbon and nitrogen metabolism in plant and algal cells. Annu Rev Plant Physiol Plant Mol Biol **45:**577–607. http://dx.doi.org/10.1146/annurev.pp.45.060194.003045.
43. **Cullen JJ.** 1985. Diel vertical migration by dinoflagellates: roles of carbohydrate metabolism and behavioral flexibility. Contrib Mar Sci **27:** 135–152.
44. **Muscatine L, Hand C.** 1958. Direct evidence for the transfer of materials from symbiotic algae to the tissues of a coelenterate. Proc Natl Acad Sci U S A **44:**1259–1263. http://dx.doi.org/10.1073/pnas.44.12.1259.
45. **Goreau TF, Goreau NI.** 1960. Distribution of labeled carbon in reef-building corals with and without zooxanthellae. Science **131:**668–669. http://dx.doi.org/10.1126/science.131.3401.668.
46. **Battey JF, Patton JS.** 1984. A reevaluation of the role of glycerol in carbon translocation in zooxanthellae-coelenterate symbiosis. Mar Biol **79:**27–38. http://dx.doi.org/10.1007/BF00404982.
47. **Swanson R, Hoegh-Guldberg O.** 1998. Amino acid synthesis in the symbiotic sea anemone *Aiptasia pulchella*. Mar Biol **131:**83–93. http://dx.doi.org/10.1007/s002270050299.
48. **Kellogg RB, Patton JS.** 1983. Lipid droplets, medium of energy exchange in the symbiotic anemone *Condylactis gigantea*: a model coral polyp. Mar Biol **75:**137–149. http://dx.doi.org/10.1007/BF00405996.
49. **Patton JS, Burris JE.** 1983. Lipid synthesis and extrusion by freshly isolated zooxanthellae (symbiotic algae). Mar Biol **75:**131–136. http://dx.doi.org/10.1007/BF00405995.
50. **Harrison PJ, Waters RE, Taylor F.** 1980. A broad spectrum, artificial sea water medium for coastal and open ocean phytoplankton. J Phycol **16:** 28–35.
51. **Gladfelter EH, Michel G, Sanfelici A.** 1989. Metabolic gradients along a branch of the reef coral *Acropora palmata*. Bull Mar Sci **44:**1166–1173.
52. **Hill R, Schreiber U, Gademann R, Larkum AWD, Kühl M, Ralph PJ.** 2004. Spatial heterogeneity of photosynthesis and the effect of temperature-induced bleaching conditions in three species of corals. Mar Biol **144:**633–640. http://dx.doi.org/10.1007/s00227-003-1226-1.
53. **Ralph PJ, Schreiber U, Gademann R, Kühl M, Larkum AWD.** 2005. Coral photobiology studied with a new imaging pulse amplitude modulated fluorometer. J Phycol **41:**335–342. http://dx.doi.org/10.1111/j.1529-8817.2005.04034.x.